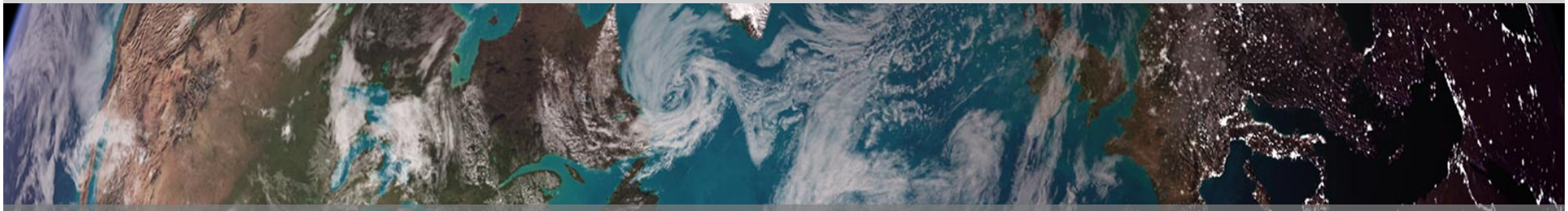

GSICS 2025 Annual Meeting

GOES 16-19 Solar and Galactic Proton Sensor (SGPS) Cross-Calibrations During Oct-Nov 2024 SEP Events

Brian T. Kress, Juan V. Rodriguez, and Athanasios Boudouridis

NOAA National Centers for Environmental Information (NCEI), Boulder, CO and
Cooperative Institute for Research in the Environmental Sciences (CIRES) at CU Boulder

GOES 16-19 Space Environment In-Situ Suite (SEISS)
Solar and Galactic Proton Sensor (SGPS)

Solar and Galactic Proton Sensor

- 2 units on each GOES-R series spacecraft, one looking east and one west (8 in total)
- 3 solid state telescopes on each unit
- 1-500 MeV protons in 13 differential channels, plus >500 MeV integral channel
- 4 MeV-500 MeV alphas in 11 energy bands
  (Included in operational data after 2022-04-25.)

GOES-R Series SGPS Proton Energy Channels by Telescope (MeV)			
SGPS Tel. 1	SGPS Tel. 2	SGPS Tel. 3	EPS/EPEAD
P1: 1.0–1.9	P6: 25–40	P8A: 83–99	P1: 0.74–4.2
P2A: 1.9–2.3	P7: 40–80	P8B: 99–118	P2: 4.2–8.7
P2B: 2.3–3.4		P8C: 118–150	P3: 8.7–14.5
P3: 3.4–6.5		P9: 150–275	P4: 15–40
P4: 6.5–12		P10: 275–500	P5: 38–82
P5: 12–25		P11: >500	P6: 84–200
			P7: 110–900

GOES 13-15 (and earlier) EPS channels shown in right column for reference, derived from cross calibrations with SEPEM energies [Sandberg et al., 2014].

SEISS SGPS designed, built, and calibrated by Assurance Technology Corporation

Start of data collection
GOES-16: 8 Jan. 2017
GOES-17: 24 April 2018
GOES-18: 25 April 2022
GOES-19: 22 August 2024
Data available at:
https://www.ncei.noaa.gov/products/satellite/goes-r

Cross calibration of Solar Energetic Particle (SEP) measurements in geostationary orbit

- **General approach**
  1. Identify periods when we expect detectors at different locations and with different look-directions to measure the same flux.
  2. Quantify systematic differences between flux measurements.
  3. May adjust geometric factors and/or energy bounds to bring reported fluxes into better agreement.
- **Criteria for comparisons**
  - Assuming an isotropic and homogeneous SEP distribution in near-Earth interplanetary space; we expect the same solar proton flux measurement, at different longitudes and look-directions, when the measured energies are above the proton cutoff energies for all directions of arrival within the detector fields-of-view and at both spacecraft locations [Kress et al., 2013; 2021; Rodriguez et al., 2014].
  - At energies below the proton cutoff energy, there are natural, geophysical differences between proton fluxes at different LTs and/or in different look directions.
- **Additional Considerations**
  - At SEP event onset, interplanetary SEP flux is often anisotropic. During the peak and declining phase, the flux usually becomes more isotropic [Reid, 1964; Desai & Giacalone, 2016].
  - During geomagnetically disturbed periods, magnetospheric shielding of interplanetary ions is suppressed allowing solar protons with energies above a few MeV unimpeded access well inside of geosynchronous. This enables cross calibration of SGPS ~2-80 MeV energy channels.

Solar Particle Events Since G19 SGPS Sensor Activation on 8/22/2024

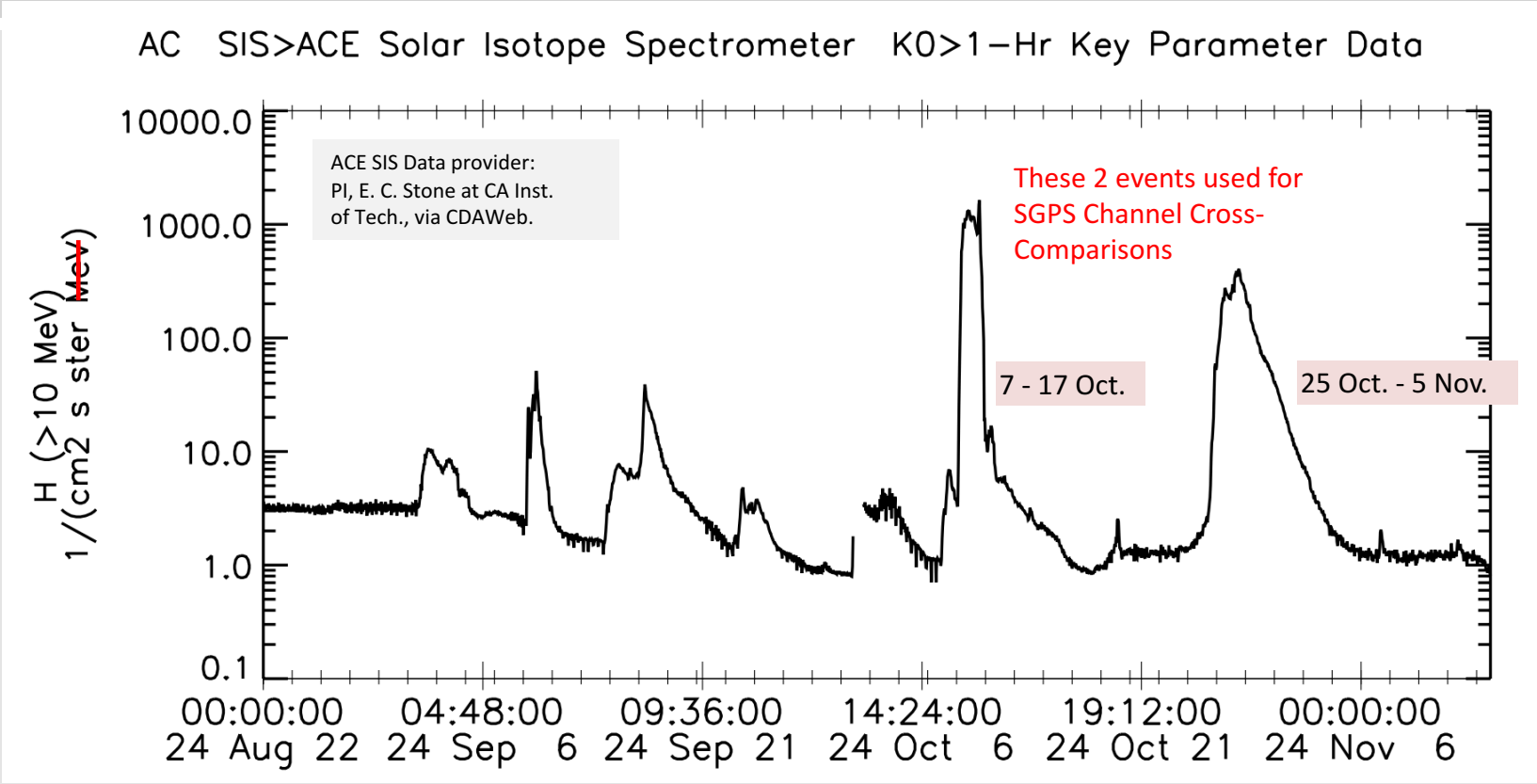

- The 7-17 October 2024 SEP event included enhancements in SGPS channels up to and including P11 (>500 MeV).
- The 25 October – 5 November 2024 SEP event included enhancements in SGPS channels up to and including P9 (150-275 MeV).

Oct-Nov 2024 Solar Particle Events

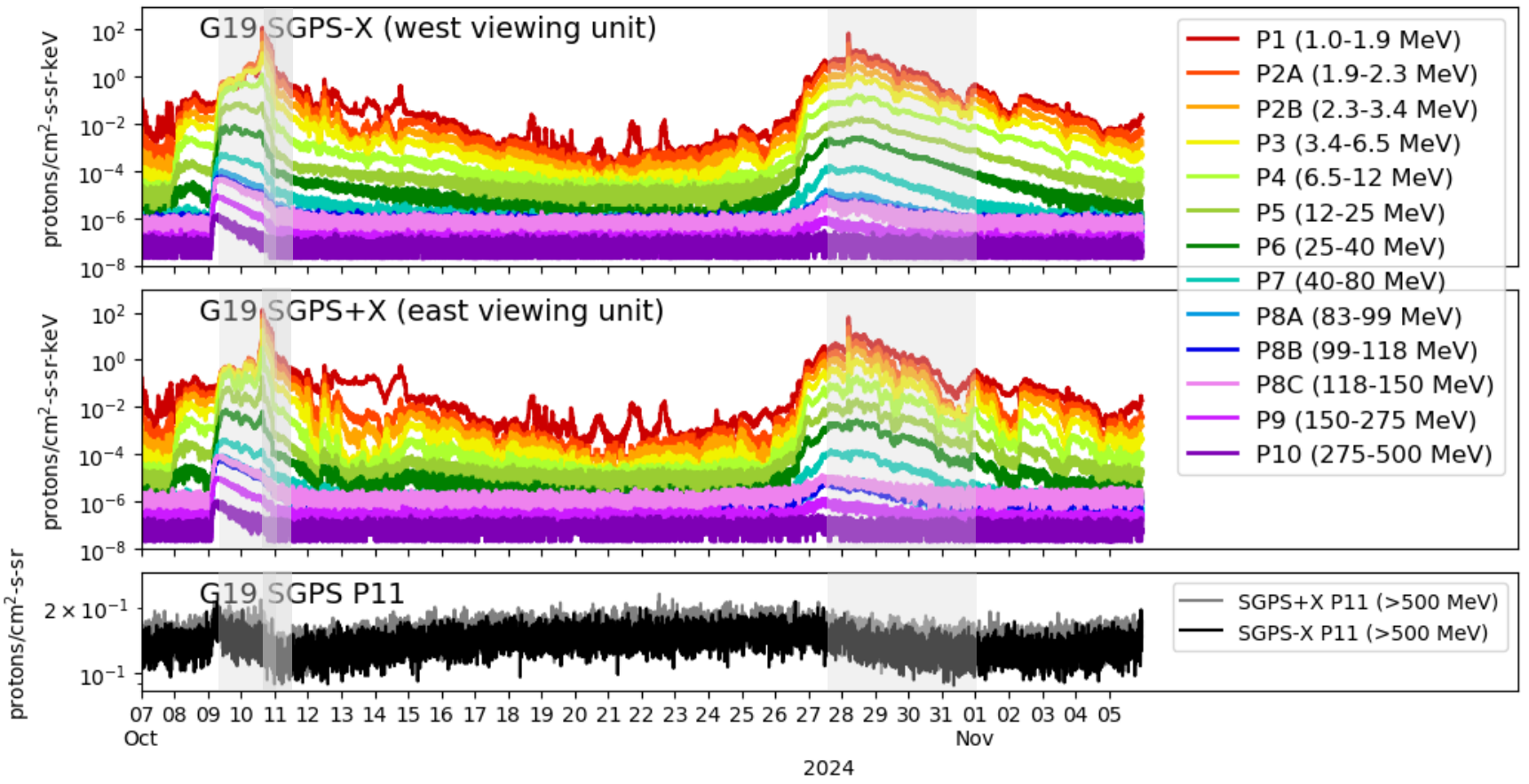

- G19 SGPS 5m averaged fluxes from 7 Oct – 5 Nov 2024.
- Gray shaded regions are periods used for G19-G16 P6-P10 cross comparisons (using 1-hour averages).
- Somewhat darker gray shaded region on 10 & 11 Oct. includes high solar wind dynamic pressure and geomagnetic storm, thus used for P1-P5 comparisons (using 5-minute averages).

Time interval for inter-calibration

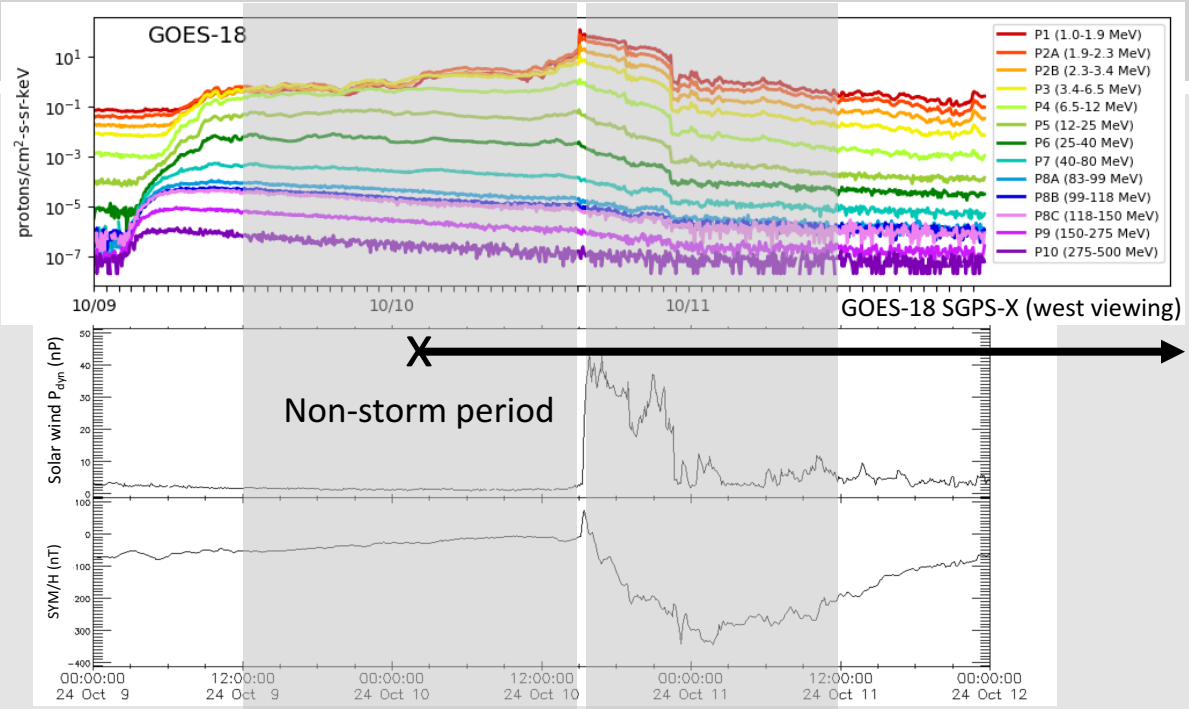

Non-storm period

OMNI data from J. H. King and N. Papatashvilli, NASA GSFC and CDAWeb

High solar wind dynamic pressure (P_{dyn}) and geomagnetic storm

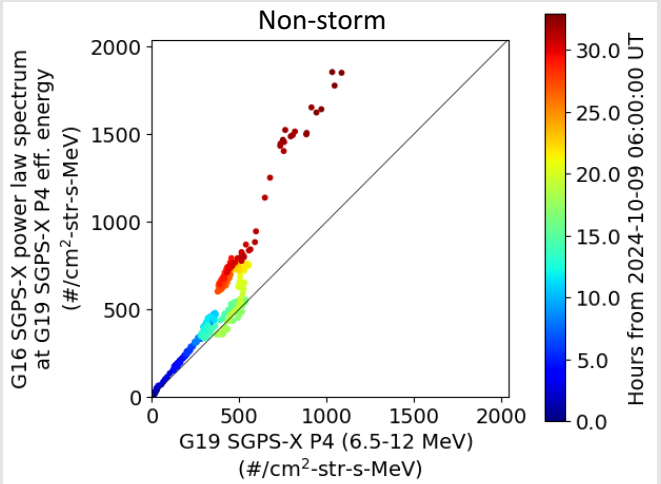

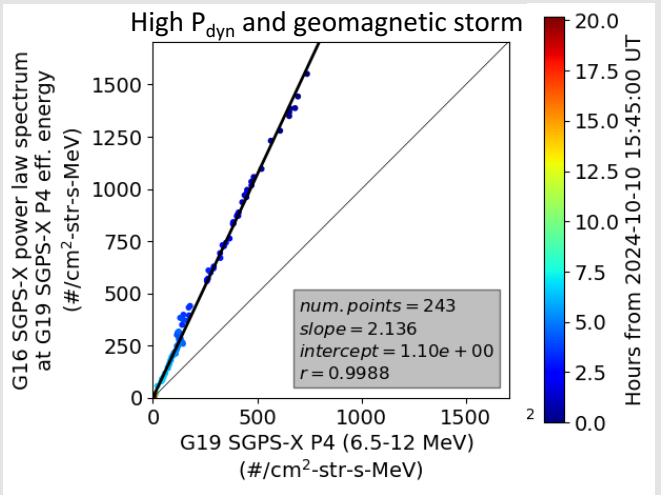

Method for cross-comparisons

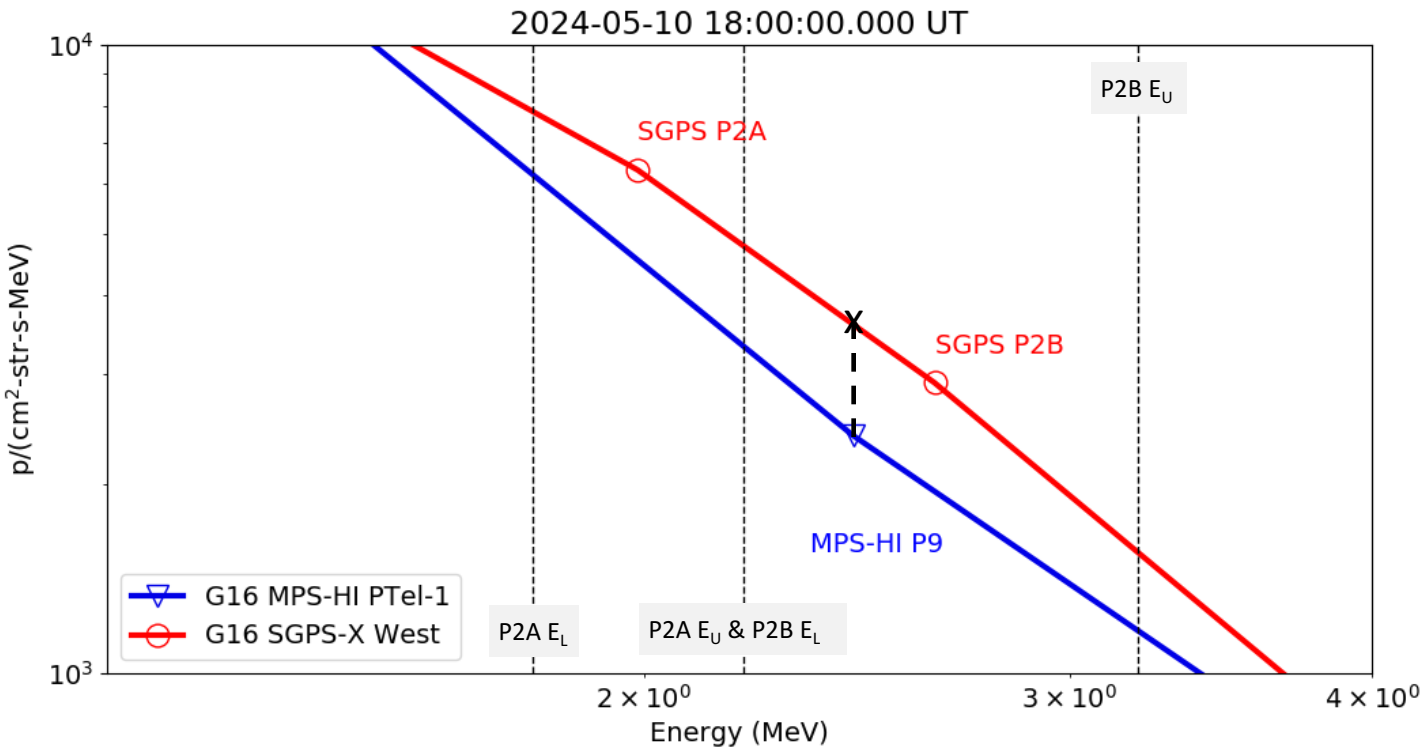

- Observed fluxes are iteratively fit to a continuous sequence of piecewise power law functions to obtain consistent spectra and channel effective energies [as in Kress et al., 2021, Sect. 5].
- In the example shown, the MPS-HI P9 flux is compared with the SGPS spectrum at the MPS-HI P9 channel effective energy.

Cross-comparison scatter plot example

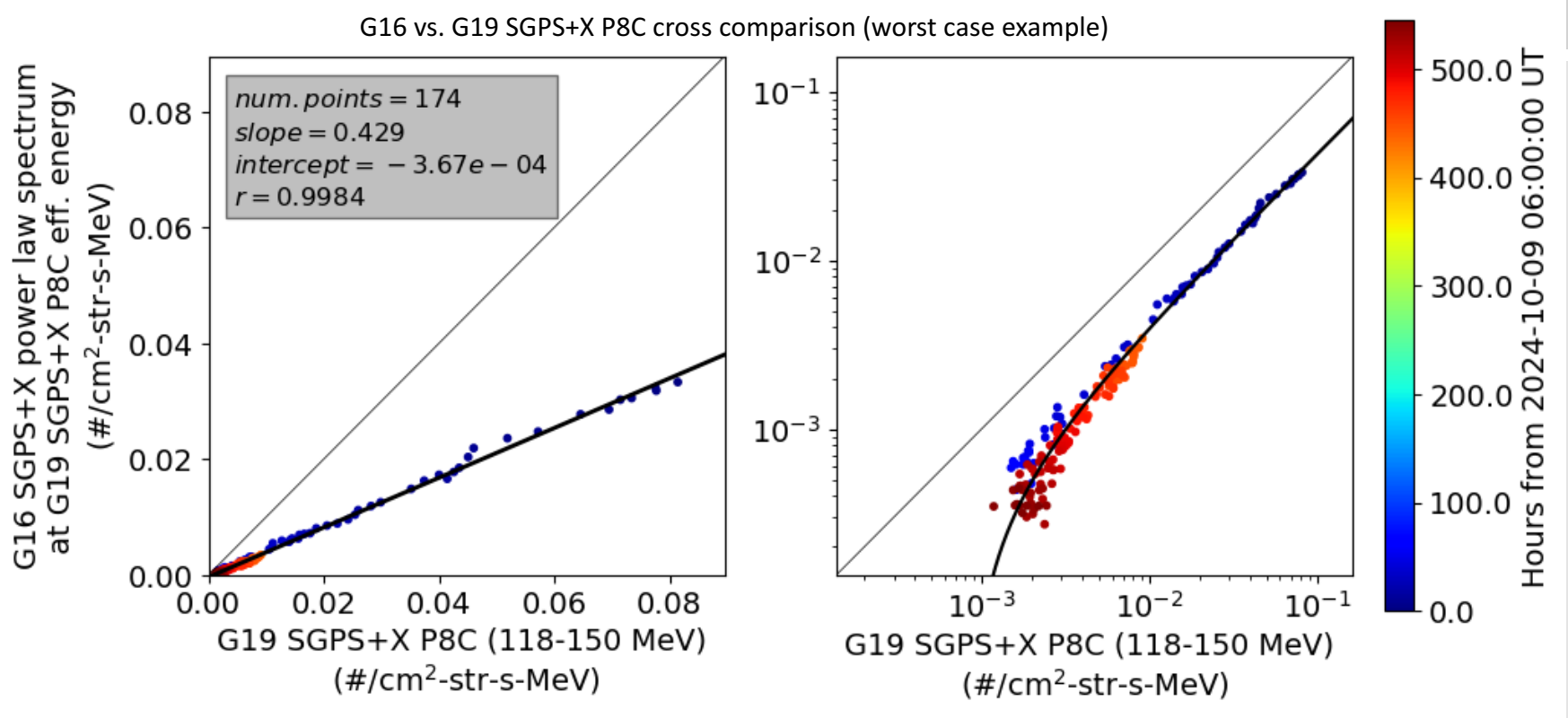

- G16-G19 SGPS+X P8C cross comparison of 1-hour averaged fluxes during Oct-Nov 2024 SPEs.
- Same data and OLS fit are shown in both panels, using linear scales on left and log scales on right.
- A power law is fit to the G16 fluxes, and comparisons with the G16 spectrum are made at G19 channel effective energies.
- Result shows a factor of ≈2.3 difference between G16 and G18 SGPS+X P8C channels.

SGPS cross comparison results

Worst case is factor of ≈2.3 difference between G16 and G18 SGPS+X P8C channels

GOES-16 SGPS-X vs. G19 SGPS-X (west viewing)

Chan.	No. Points	Slope	Intercept	r-value
P1	235	0.844	-2.49E+01	0.9994
P2A	243	0.681	1.33E+02	0.9969
P2B	243	0.949	-7.09E+00	0.9991
P3	243	0.811	-1.32E+01	0.9988
P4	243	2.136	1.10E+00	0.9988
P5	243	1.446	-3.94E-01	0.9984
P6	174	0.617	-9.66E-03	0.9976
P7	174	0.929	-2.10E-03	0.9982
P8A	174	1.08	-1.05E-04	0.999
P8B	174	1.118	-8.01E-05	0.9992
P8C	173	0.639	-2.64E-05	0.9923
P9	174	0.958	-7.15E-06	0.998
P10	173	1.075	-1.69E-05	0.9914
P11	174	1.036	2.64E-03	0.9062

GOES-16 SGPS+X vs. G19 SGPS+X (east viewing)

Chan.	No. Points	Slope	Intercept	r-value
P2A	243	1.186	6.97E+01	0.9992
P2B	243	0.918	-1.67E+01	0.9995
P3	243	0.899	-2.64E+01	0.9991
P4	243	0.736	-2.89E+00	0.9991
P5	243	0.788	-1.55E-01	0.9989
P6	174	0.881	-1.60E-02	0.9991
P7	174	0.911	-8.29E-03	0.9853
P8A	174	1.115	1.57E-05	0.9995
P8B	174	0.914	-1.80E-04	0.9994
P8C	174	0.429	-3.67E-04	0.9984
P9	174	0.962	-3.93E-05	0.9995
P10	174	1.25	-1.54E-05	0.9854
P11	174	0.808	2.67E-02	0.865

- Measurements from like channels and look-directions generally agree to within 10-30%.
- Worst case is ~130% error in G19 SGPS+X P8C (taking G16 flux as “accepted” value).

Cross sensor comparison P1-P5 overview

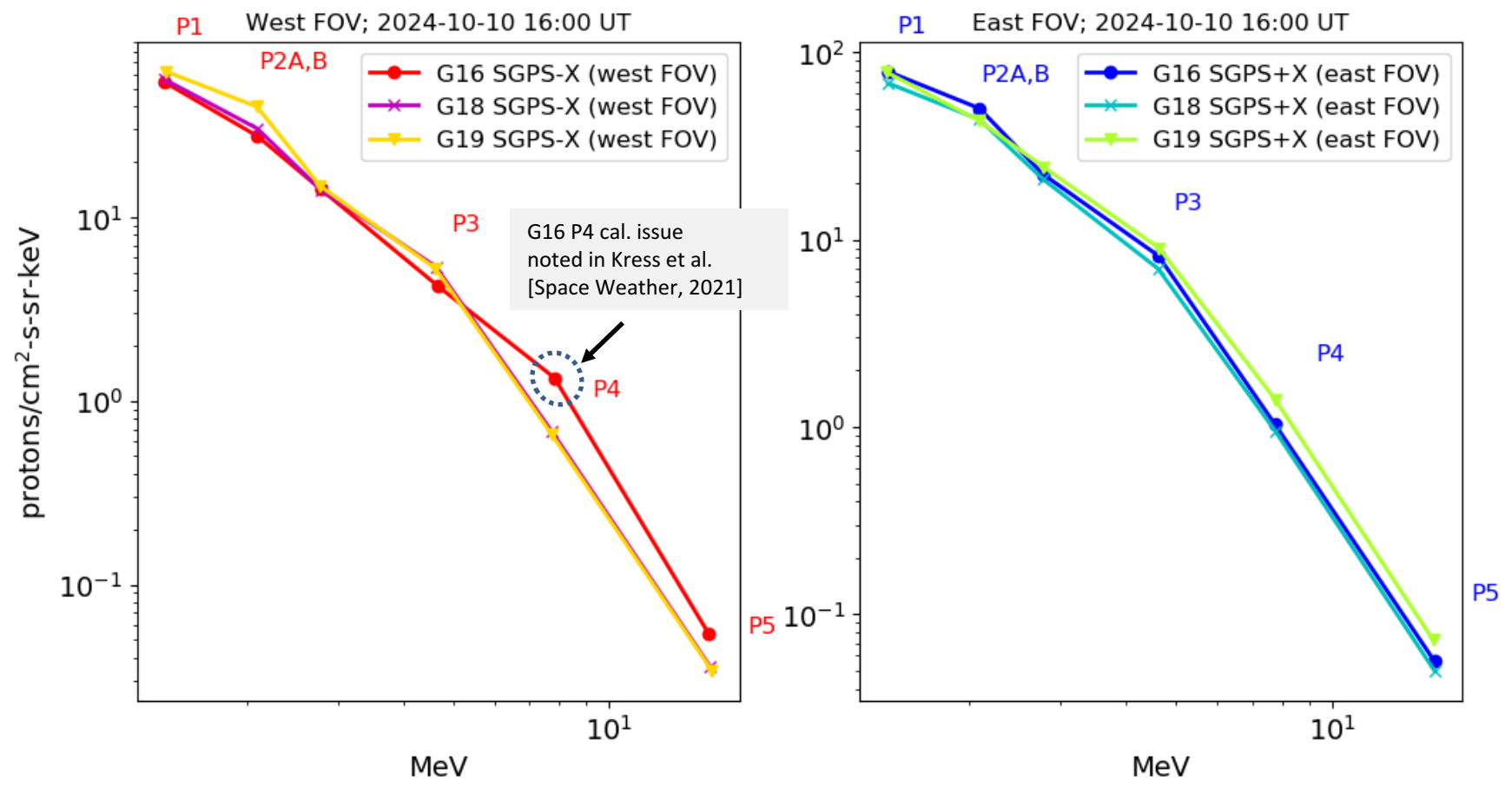

- G16 and G19 SGPS 1-hour averaged spectra from 16-17 UT on 10 Oct 2024.
- Agreement is expected between SEP fluxes measured at different longitudes and in different look directions due to high solar wind dynamic pressure and geomagnetic storm during this period.

Cross sensor comparison P6-P10 overview

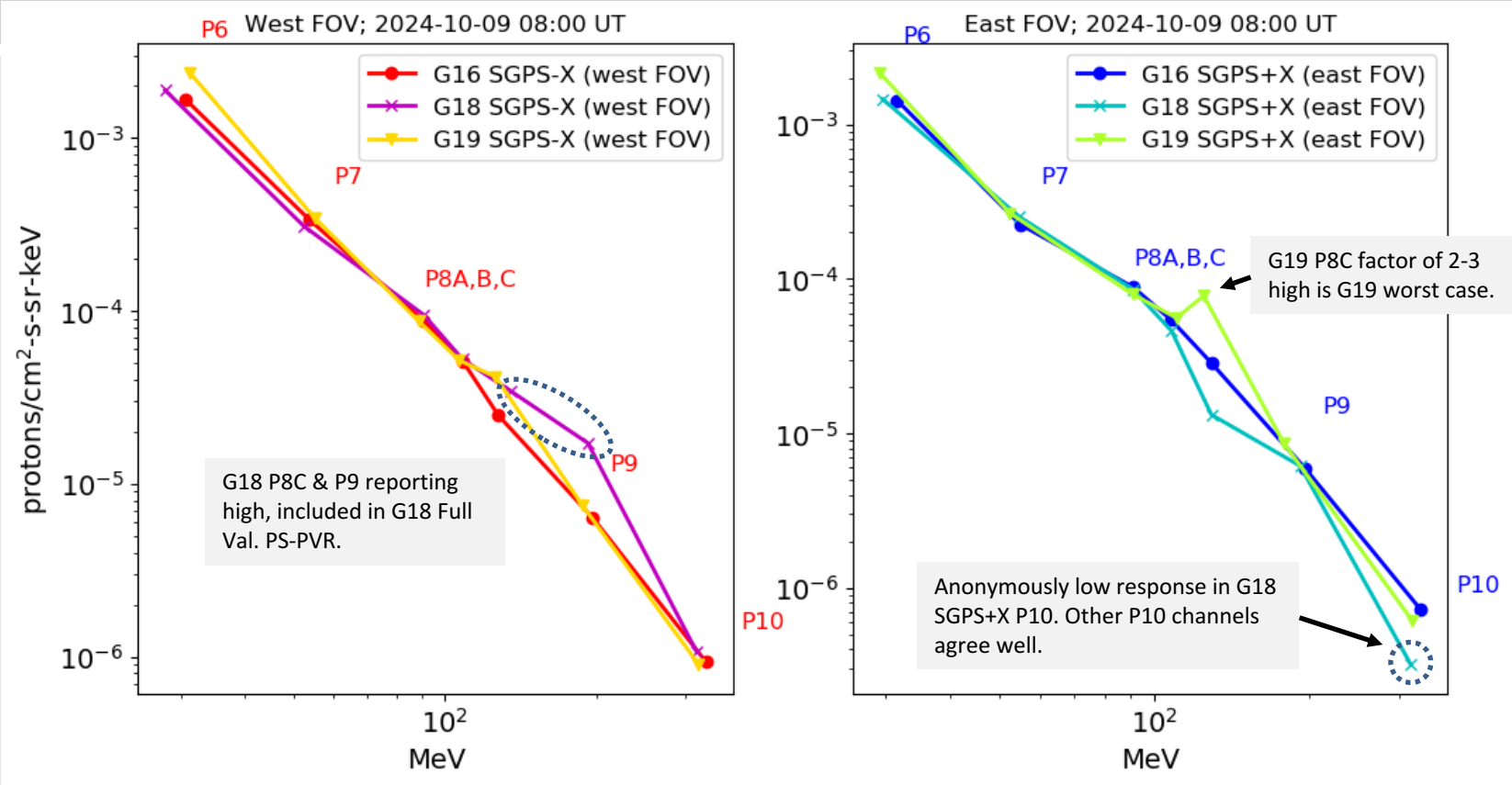

- G16 and G19 SGPS 1-hour averaged spectra from 8-9 UT on 9 Oct 2024.
- Agreement is expected between SEP fluxes measured at different longitudes and in different look directions since energies >80 MeV are not geomagnetically shielded at geosynchronous, and the interplanetary SEP distribution is isotropic following the event peak during this event.

Summary of SGPS anomalous channels

- Temperature dependent channels
  - G16 SGPS-X P2A-P5, P8C-P11
  - G18 SGPS+X P8C-P11
- Reporting low/high ($\gtrsim$ factor of 2)
  - G16 SGPS-X P4 reporting high;
  - G17 SGPS+X P8C reporting high
  - G18 SGPS-X P8C and P9 reporting high
  - G18 SGPS+X P8C and P10 reporting low
  - G19 SGPS+X P8C reporting high

Summary

- Inter-calibrations among solar particle sensors aid in identifying and understanding measurement discrepancies, potentially correcting errors, and ultimately improving space-based particle detector systems.
- The GOES-R series SGPS inter-calibrations exploit periods when similar flux measurements are expected in both detectors to identify and correct instrument and/or calibration anomalies.
- Our present goal is to characterize systematic differences between similar channels.
- Cross calibration of $\gtrsim$40-80 MeV channels is possible when the interplanetary SEP distribution becomes isotropic and homogeneous (usually after event peak flux).
- Geomagnetic storms and periods of high solar wind dynamic pressure enable cross calibration of proton channels in the 2-40 MeV range.
- A series of solar particle events since GOES-19 SGPS began collecting data on 22 August 2024 enable comprehensive comparisons between GOES-16, -18 and -19 SGPS units.
- The results of this work will guide future adjustments of calibration factors.

References

Desai, M., & Giacalone, J. (2016). Large gradual solar energetic particle events. Living Reviews in Solar Physics, 13, 3. https://doi.org/10.1007/s41116-016-0002-5

Kress, B. T., Rodriguez, J. V., Mazur, J. E., & Engel, M. (2013). Modeling solar proton access to geostationary spacecraft with geomagnetic cutoffs. *Journal of Advance Space Research*, *52*, 1939–1948. https://doi.org/10.1016/j.asr.2013.08.019

Kress, B. T., Rodriguez, J. V., Boudouridis, A., Onsager, T. G., Dichter, B. K., Galica, G. E., & Tsui, S. (2021). Observations from NOAA's newest solar proton sensor. *Space Weather*, *19*, e2021SW002750. https://doi.org/10.1029/2021SW002750

Reid, G. C. (1964). A diffusive model for the initial phase of a solar proton event. Journal of Geophysical Research, 69(13), 2659–2667. https://doi.org/10.1029/JZ069i013p02659

Rodriguez, J. V., Krosschell, J. C., & Green, J. C. (2014). Intercalibration of GOES 8-15 solar proton detectors. *Space Weather*, *12*, 92–109. https://doi.org/10.1002/2013SW000996

Rodriguez, J.V., Kress, B.T., 2023. GOES observations of solar protons during ground level enhancements, in: NMDB@Athens: Proceedings of the Hybrid Symposium on Cosmic Ray Studies with Neutron Detectors, September 26-30, 2022, Cosmic Ray Studies with Neutron Detectors. pp. 69–80. https://doi.org/10.38072/2748-3150/p32

Sandberg, I., Jiggens, P., Heynderickx, D., & Daglis, I. A. (2014). Cross calibration of NOAA GOES solar proton detectors using corrected NASA IMP-8/GME data. *Geophysical Research Letters, 41*, 4435–4441. https://doi.org/10.1002/2014GL060469